

The $\psi_o = \text{constant}$ Mode in Free-Space and Conical Waveguides

J. Van Bladel

Abstract— $\psi_o = \text{constant}$ is one of the Neumann eigenfunctions used to expand the axial \mathbf{H} component in a cylindrical waveguide. It cannot be omitted, lest erroneous results are obtained in, for example, aperture coupling with the exterior region. This paper investigates whether the same situation holds for a conical waveguide, and extends the analysis to free space, which may be considered as a radial waveguide.

Index Terms—Aperture coupling, multipole expansion, waveguides.

I. INTRODUCTION

Recent papers [1], [2] show continuing interest in the spherical multipole expansion of transient fields. It is, therefore, appropriate to investigate whether a field behavior that exists in a cylindrical waveguide may be extended to the *radial* waveguide formed by free space. The behavior in question concerns the expansion of H_z in a cylindrical waveguide in terms of the Neumann eigenfunctions ψ_{mn} of the cross section (Fig. 1). One of these (normalized) eigenfunctions is the constant $\psi_o = (1/\sqrt{S})$. Its contribution may *not* be ignored in the expansion, although the (x, y) gradient of ψ_o vanishes; hence, does not contribute to the transverse components of either \mathbf{E} or \mathbf{H} . Since the other Neumann eigenfunctions have zero average value over S (a result of the well-known orthogonality properties of ψ_{mn}) the $\psi_o = (1/\sqrt{S})$ term is responsible for the average value of H_z over the cross section. Simple manipulations show that under time-harmonic conditions [3]

$$(H_z)_{\text{ave}} = -\frac{1}{j\omega\mu_0}(\mathbf{u}_z \cdot \mathbf{J}_m)_{\text{ave}} - \frac{1}{j\omega\mu_0 S} \int_c \mathbf{u}_z \cdot (\mathbf{u}_n \times \mathbf{E}) dc. \quad (1)$$

This term, therefore, exists only in the presence of *volume* magnetic currents (such as the magnetic equivalent of a small electric current loop) or *surface* magnetic currents (such as the $\mathbf{u}_n \times \mathbf{E}$ field in the S_a aperture). It should be emphasized that the contribution (1) is not an intellectual nicety, but an important factor in the investigation of field coupling through the waveguide aperture S_a . The method is well known: $\mathbf{u}_n \times \mathbf{E}$ is assumed given in S_a , $\mathbf{H} \times \mathbf{u}_n$ is expressed in terms of $\mathbf{u}_n \times \mathbf{E}$ on both sides of S_a , and $\mathbf{H} \times \mathbf{u}_n$ is required to be continuous across the aperture. In this process, which results in an integral equation for $\mathbf{u}_n \times \mathbf{E}$, the z -component of \mathbf{H} intervenes since $\mathbf{u}_c \cdot (\mathbf{H} \times \mathbf{u}_n) = H_z$. Fig. 2 shows the error that may appear when the ψ_o term is omitted [4]. This figure evidences a behavior that could have been deduced from (1) since $(H_z)_{\text{ave}}$ exists only “under the aperture.” As a result, no energy is radiated by the “mode” (hence, the lack of influence of ψ_o on the resistance), while reactive energy is generated (hence, the influence of ψ_o on the reactance).

Relationship (1) can be rewritten in terms of the flux Φ_m of \mathbf{B} through a cross section. Thus,

$$-j\omega\Phi_m = \int_S \mathbf{J}_{mz} dS + \int_c (\mathbf{u}_c \cdot \mathbf{E}) dc. \quad (2)$$

Manuscript received October 31, 2000.

The author is with the Department of Information Technology, University of Ghent, Gent B9000, Belgium.

Publisher Item Identifier S 0018-9480(02)03026-0.

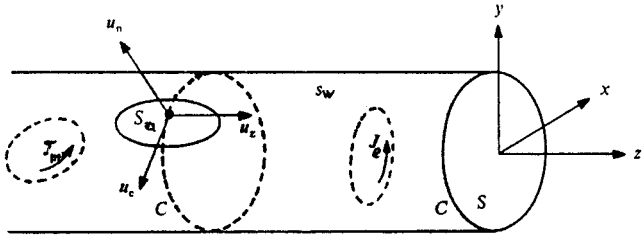
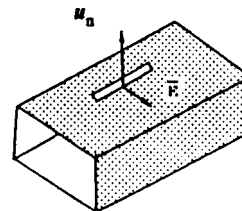
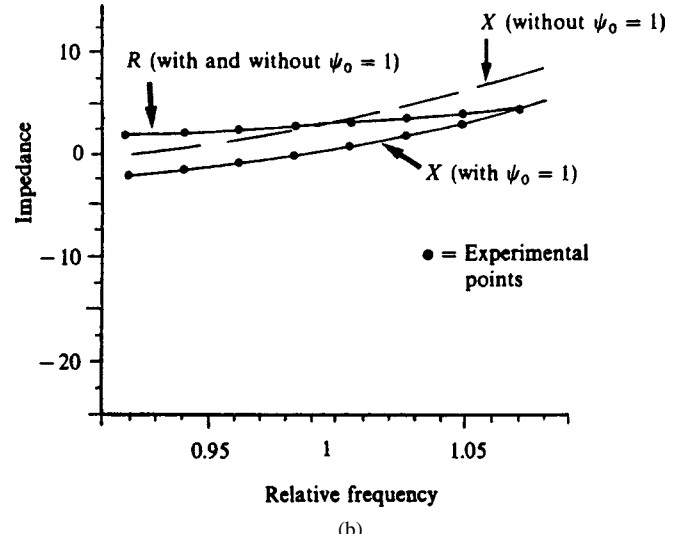


Fig. 1. Waveguide with electric and magnetic sources.



(a)



Relative frequency

(b)

Fig. 2. (a) Slot in a rectangular waveguide. (b) Theoretical and experimental results for shunt impedance of a rectangular slot (communicated by R. W. Lyon).

This flux is not conservative, a not too surprising property since $\text{div } \mathbf{B} = \rho_m \neq 0$ in the presence of volume currents \mathbf{J}_m and since flux can escape from (or penetrate through) the aperture in the wall.

II. EIGENVECTORS FOR A CONICAL WAVEGUIDE

The field expansion in a conical waveguide is based on two sets of eigenfunctions. Both of these are defined on S_1 , the intersection of the conical volume with a spherical surface of unit radius (Fig. 3). The Dirichlet eigenfunctions $\phi_m(\theta, \omega)$ are defined by the relationships

$$\begin{aligned} \nabla_1^2 \phi_m + k_m^2 \phi_m &= 0, & \text{in } S_1 \\ \phi_m &= 0, & \text{on } C_1 \end{aligned} \quad (3)$$

where ∇_1^2 is the Laplacian on the unit surface S_1 , viz

$$\nabla_1^2 \phi_m = \nabla_{\theta, \varphi}^2 \phi_m = \frac{1}{\sin \theta} \frac{\partial}{\partial \theta} \left(\sin \theta \frac{\partial \phi_m}{\partial \theta} \right) + \frac{1}{\sin^2 \theta} \frac{\partial^2 \phi_m}{\partial \varphi^2}. \quad (4)$$

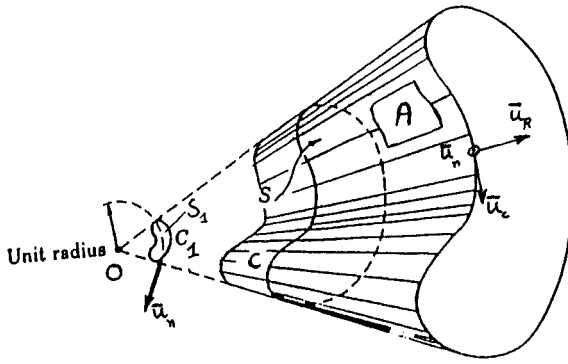


Fig. 3. Conical waveguide with aperture in the wall.

Here, and in the sequel, we use subscript “1” to denote an operator involving only the θ and φ coordinates. The index m is a concise notation for a double index. The Neumann eigenfunctions, on the other hand, satisfy

$$\begin{aligned} \nabla_1^2 \psi_p + k_p^2 \psi_p &= 0, & \text{in } S_1 \\ \frac{\partial \psi_p}{\partial n} &= 0, & \text{on } C_1. \end{aligned} \quad (5)$$

The direction n , shown in Fig. 3, is perpendicular to the outer wall, i.e., to the tangent plane formed by \mathbf{u}_R and \mathbf{u}_c . More specifically, $\mathbf{u}_n = \mathbf{u}_c \times \mathbf{u}_R$. On the basis of a well-known Green’s theorem [5]

$$\int_{S_1} (a \nabla_1^2 b - b \nabla_1^2 a) d\Omega = \int_{C_1} \left(a \frac{\partial b}{\partial n} - b \frac{\partial a}{\partial n} \right) dc \quad (6)$$

where $d\Omega = \sin \theta \, d\theta \, d\varphi$, it is easy to show that ϕ_m forms an orthogonal set with respect to the real scalar product

$$\langle a, b \rangle_1 = \int_{S_1} ab \, d\Omega. \quad (7)$$

The same holds for ψ_p . We shall assume that both sets are normalized. In the Neumann family, the normalized constant $\Psi_o = (1/\sqrt{S_1})$, which may *not* be omitted, can also be written in the form $(1/\sqrt{\Omega})$, where Ω is the solid angle filled by the conical volume. It is interesting to note *en passant* that k_m and k_p appear in the study of the field singularities at the tip of a metallic cone. In fact, their lowest value determines the strength of the singularity. Relevant numerical data are available in [4] for a few typical cross sections.

Germaine to the field expansion are the eigenvectors related to ϕ_m and ψ_p . These are $\text{grad}_1 \phi_m$ and $\text{grad}_1 \psi_p$, where

$$\text{grad}_1 a(\theta, \varphi) = \frac{\partial a}{\partial \theta} \mathbf{u}_\theta + \frac{1}{\sin \theta} \frac{\partial a}{\partial \varphi} \mathbf{u}_\varphi. \quad (8)$$

Introducing a scalar product

$$\langle \mathbf{a}, \mathbf{b} \rangle = \int_{S_1} \mathbf{a} \cdot \mathbf{b} \, d\Omega \quad (9)$$

and taking Green’s theorem

$$\int_{S_1} \left(a \nabla_1^2 b + \text{grad}_1 a \cdot \text{grad}_1 b \right) d\Omega = \int_{C_1} a \frac{\partial b}{\partial n} dc \quad (10)$$

into account, it is a simple matter to show that the family $\text{grad}_1 \phi_m$ forms an orthogonal set. The norm of these vectors is related to the norm of ϕ_m by (10), which gives

$$\int_{S_1} |\text{grad}_1 \phi_m|^2 d\Omega = k_m^2 \int_{S_1} \phi_m^2 d\Omega = k_m^2. \quad (11)$$

The $\text{grad}_1 \phi_m$ vectors are perpendicular to C_1 . The vectors $\mathbf{u}_R \times \text{grad}_1 \phi_m$ also form an orthogonal set, with the same norm. The two sets are mutually orthogonal since [5]

$$\int_{S_1} \text{grad}_1 a \cdot (\mathbf{u}_R \times \text{grad}_1 b) d\Omega = - \int_{C_1} a \mathbf{u}_c \cdot \text{grad}_1 b dc \quad (12)$$

and the line integral vanishes for $a = b = \phi_m$. The two sets have separate purposes, as can be seen by writing the Helmholtz theorem on the sphere in the form [5]

$$\mathbf{a}(\theta, \varphi) = \text{grad}_1 \phi + \mathbf{u}_R \times \text{grad}_1 \psi \quad (13)$$

where \mathbf{a} is a vector tangent to S_1 . Clearly, $\text{grad} \phi_m$ are suitable to expand the $\text{grad}_1 \phi$ term, and $\mathbf{u}_R \times \text{grad}_1 \phi_m$ are suitable to expand the $\mathbf{u}_R \times \text{grad}_1 \psi$ term.

A similar analysis shows that $\text{grad}_1 \psi_p$ form an orthogonal set, with norm (11), where k_m^2 should be replaced by k_p^2 . Further, the $\mathbf{u}_R \times \text{grad}_1 \psi_p$ form another orthogonal set. From (12), these sets are mutually orthogonal, and there is cross-orthogonality between $\text{grad}_1 \phi_m$ and $\mathbf{u}_R \times \text{grad}_1 \psi_p$. In Section III, we shall use these properties to expand the fields in an arbitrary cross section S , part of a spherical surface of radius R . The suitable eigenvectors are now $\text{grad}_s \phi_m$ and $\text{grad}_s \psi_p$, e.g.,

$$\text{grad}_s \phi_m(\theta, \varphi) = \frac{1}{R} \frac{\partial \phi_m}{\partial \theta} \mathbf{u}_\theta + \frac{1}{R \sin \theta} \frac{\partial \phi_m}{\partial \varphi} \mathbf{u}_\varphi = \frac{1}{R} \text{grad}_1 \phi_m. \quad (14)$$

Orthogonality is now with respect to the scalar product

$$\langle \mathbf{a}, \mathbf{b} \rangle = \int_S (\mathbf{a} \cdot \mathbf{b}) dS \quad (15)$$

where $dS = R^2 d\Omega$. The normalized eigenfunctions are ϕ_m/R and ψ_p/R , including $\psi_o/R = 1/\sqrt{S_1} = 1/R\sqrt{\Omega}$. Thus,

$$\begin{aligned} \int_S |\text{grad}_s \phi_m|^2 R^2 d\Omega &= \int_{S_1} |\text{grad}_1 \phi_m|^2 d\Omega = k_m^2 \\ \int_S \left(\frac{\phi_m}{R} \right)^2 R^2 d\Omega &= \int_{S_1} \phi_m^2 d\Omega = 1. \end{aligned}$$

III. FIELD EXPANSION IN A CONICAL REGION

Since the electric field is perpendicular to the boundary wall (except in the aperture, if there is one) it is natural to expand \mathbf{e} in eigenvectors that partake of the same property. Such a move will improve convergence. We write

$$\mathbf{e}(\mathbf{r}, t) = \sum_m v_m(R, t) \text{grad}_s \phi_m + \sum_p v_p(R, t) \text{grad}_s \psi_p \times \mathbf{u}_R. \quad (16)$$

The magnetic field, which is tangent to the metal, will similarly be expanded as

$$\begin{aligned} \mathbf{h}(\mathbf{r}, t) &= \sum_m i_m(R, t) \mathbf{u}_R \times \text{grad}_s \phi_m + \sum_p i_p(R, t) \text{grad}_s \psi_p \\ &+ \sum_{p \neq o} \ell_p(R, t) \frac{1}{R} \psi_p \mathbf{u}_R + \ell_o(R, t) \frac{1}{R\sqrt{\Omega}} \mathbf{u}_R. \end{aligned} \quad (17)$$

The volume source terms must also be expanded, \mathbf{j}_e in terms of the eigenfunctions and eigenvectors used for \mathbf{e} , \mathbf{j}_m in terms of those used for \mathbf{h} . The various expansions must now be inserted into Maxwell’s equations, and the coefficients equated on both sides of the equations. In the absence of an aperture, $\text{curl } \mathbf{e}$ will simply be the sum of the curls of the terms in the right-hand-side member. In the presence of an aperture, however, \mathbf{e} does not satisfy everywhere the boundary conditions satisfied by the eigenvectors, and “the derivative of the sum” will not be

equal to the “sum of the derivatives.” This is a classic difficulty, which is remedied by introducing separate expansions for curl_s and curl_h . A typical derivation is given in the Appendix.

It is well known that the total field can be split into partial TE and TM modes, which, respectively, involve the “ p ” and “ m ” coefficients. Although this paper concentrates on the $\ell_o(R, t)$ coefficient, all coefficients of the TE mode will nevertheless be considered, for the sake of completeness. They satisfy the differential system

$$\begin{aligned} \frac{\partial v_p}{\partial R} + \mu_o \frac{\partial i_p}{\partial t} &= -\frac{1}{k_p^2} \int_s \mathbf{j}_m \cdot \text{grad}_s \psi_p dS \\ &\quad - \frac{1}{k_p^2} \int_c (\mathbf{u}_n \times \mathbf{e}) \cdot \text{grad}_s \psi_p dc \\ &= A_p(R, t) \end{aligned} \quad (18)$$

$$\begin{aligned} \frac{\partial i_p}{\partial R} + \varepsilon_o \frac{\partial v_p}{\partial t} - \frac{1}{R} \ell_p &= -\frac{1}{k_p^2} \int_s \mathbf{j}_e \cdot (\text{grad}_s \psi_p \times \mathbf{u}_R) dS \\ &= B_p(R, t) \end{aligned} \quad (19)$$

$$\begin{aligned} k_p^2 \frac{v_p}{R} + \mu_o \frac{\partial \ell_p}{\partial t} &= - \int_s \mathbf{j}_m \cdot \mathbf{u}_R \frac{\psi_p}{R} dS \\ &\quad - \int_c (\mathbf{u}_n \times \mathbf{e}) \cdot \mathbf{u}_R \frac{\psi_p}{R} dc \\ &= C_p(R, t) \end{aligned} \quad (20)$$

$$\begin{aligned} \mu_o \frac{\partial \ell_o}{\partial t} &= -\frac{1}{R\sqrt{\Omega}} \int_s (\mathbf{j}_m \cdot \mathbf{u}_R) dS \\ &\quad - \frac{1}{R\sqrt{\Omega}} \int_c (\mathbf{u}_n \times \mathbf{e}) \cdot \mathbf{u}_R. \end{aligned} \quad (21)$$

The second members show that $\mathbf{u}_n \times \mathbf{e}$ has the nature of a surface magnetic current, in harmony with the classical theory of equivalent sources. Turning to the solution of the term in ℓ_o , we note that it yields the average radial component of \mathbf{h} over the cross section. Thus,

$$\frac{\ell_o(r, t)}{R\sqrt{\Omega}} = [h_R(R, t)]_{\text{ave}}. \quad (22)$$

The radial magnetic flux is now

$$-\frac{\partial \phi_m(R, t)}{\partial t} = \int_s (\mathbf{j}_m \cdot \mathbf{u}_R) dS + \int_c (\mathbf{u}_n \times \mathbf{e}) \cdot \mathbf{u}_R dc. \quad (23)$$

This is the time-dependent equivalent of (2). To proceed with the solution of (18)–(20), it is appropriate to eliminate i_p and ℓ_p to obtain for the principal mode function v_p

$$\begin{aligned} \frac{\partial^2 v_p}{\partial R^2} - \frac{1}{c_o^2} \frac{\partial^2 v_p}{\partial t^2} - \frac{k_p^2}{R^2} v_p &= \frac{\partial A_p(R, t)}{\partial R} \\ &\quad - \mu_o \frac{\partial B_p(R, t)}{\partial t} - \frac{1}{R} C_p(R, t). \end{aligned} \quad (24)$$

This equation is of the “spherical transmission line” type. The second member represents the coupling of the \mathbf{j}_e and \mathbf{j}_m sources to the mode. In the time-harmonic regime, the solution outside the sources is a combination of spherical Bessel functions.

For the TM modes, the equations corresponding to (18)–(20) are

$$\begin{aligned} \frac{\partial v_m}{\partial R} + \mu_o \frac{\partial i_m}{\partial t} - \frac{1}{R} w_m &= -\frac{1}{k_m^2} \int_s \mathbf{j}_m \cdot (\mathbf{u}_R \times \text{grad}_s \phi_m) dS \\ &\quad - \frac{1}{k_m^2} \int_c (\mathbf{u}_n \times \mathbf{e}) \cdot (\mathbf{u}_R \times \text{grad}_s \phi_m) dc \\ &= B_m(R, t) \end{aligned} \quad (25)$$

$$\begin{aligned} \frac{\partial i_m}{\partial R} + \varepsilon_o \frac{\partial v_m}{\partial t} &= -\frac{1}{k_m^2} \int_s \mathbf{j}_e \cdot \text{grad}_s \phi_m dS \\ &= A_m(R, t) \end{aligned} \quad (26)$$

$$k_m^2 \frac{i_m}{R} + \varepsilon_o \frac{\partial w_m}{\partial t} = - \int_s \mathbf{j}_e \cdot \mathbf{u}_R \frac{\phi_m}{R} dS = C_m(R, t). \quad (27)$$

Elimination gives a differential equation for the principal mode function i_m , viz

$$\begin{aligned} \frac{\partial^2 i_m}{\partial R^2} - \frac{1}{c_o^2} \frac{\partial^2 i_m}{\partial t^2} - \frac{k_m^2}{R^2} i_m &= \frac{\partial A_m(R, t)}{\partial R} - \varepsilon_o \frac{\partial B_m(R, t)}{\partial t} \\ &\quad - \frac{1}{R} C_m(R, t). \end{aligned} \quad (28)$$

IV. FIELD EXPANSION IN FREE SPACE

In the absence of conical conducting boundaries, the distinction between ψ_p and ϕ_m disappears, and the expansion is now in terms of the normalized eigenfunctions

$$Y_{mn}(\theta, \varphi) = \underbrace{\left[\varepsilon_m \frac{(2n+1)(n-m)!}{4\pi(n+m)!} \right]^{1/2}}_{C_{mn}} P_n^m(\cos \theta) \begin{bmatrix} \sin m\varphi \\ \cos m\varphi \end{bmatrix}. \quad (29)$$

These eigenfunctions satisfy

$$\nabla_1^2 Y_{mn}(\theta, \varphi) + n(n+1)Y_{mn}(\theta, \varphi) = 0 \quad (30)$$

where n is an integer. The basic domain S_1 is the total solid angle 4π . The functions in $\sin m\varphi$ and $\cos m\varphi$ generate “odd” and “even” modes, respectively. The eigenfunction corresponding to $n = 0, m = 0$ is the constant $1/\sqrt{4\pi}$. The eigenvectors on S_1 are now $\text{grad}_1 Y_{mn}$ and $\mathbf{u}_R \times \text{grad}_1 Y_{mn}$, where both even and odd families must be included. For the even Y_{nm} , e.g.,

$$\begin{aligned} \text{grad}_1 Y_{mn} &= C_{nm} \left\{ -\sin \theta \left[P_n^m(\cos \theta) \right]' \cos m\varphi \mathbf{u}_\theta \right. \\ &\quad \left. - \frac{m}{\sin \theta} P_n^m(\cos \theta) \sin m\varphi \mathbf{u}_\varphi \right\} \end{aligned} \quad (31)$$

where $[P_n^m(x)]' = (d P_n^m(x)/dx)$. The odd eigenvectors follow by replacing $m\varphi$ by $(m\varphi - \pi/2)$. These eigenvectors form a complete orthogonal set with norm

$$\int_{4\pi} |\text{grad}_1 Y_{mn}|^2 d\Omega = n(n+1). \quad (32)$$

The fields belong again to TE and TM families. In the TE family

$$\begin{aligned} \mathbf{e}(\mathbf{r}, t) &= \sum_{mn} v_{mn}(R, t) \text{grad}_s Y_{mn} \times \mathbf{u}_R \\ \mathbf{h}(\mathbf{r}, t) &= \sum_{m,n} i_{mn}(R, t) \text{grad}_s Y_{mn} + \sum_{m,n} \ell_{mn}(R, t) \frac{1}{R} Y_{mn} \mathbf{u}_R \\ &\quad + \ell_o \frac{1}{R\sqrt{4\pi}} \mathbf{u}_R. \end{aligned} \quad (33)$$

Insertion in Maxwell's equations yields (18)–(26), but without source terms in $(\mathbf{u}_n \times \mathbf{e})$. In addition, k_p^2 must be replaced by $n(n+1)$ and $R\sqrt{\Omega}$ by $R\sqrt{4\pi}$. The ℓ_o coefficient, for example, must now satisfy

$$\mu_o \frac{\partial \ell_o}{\partial t} = -\frac{1}{R\sqrt{4\pi}} \int_s (\mathbf{j}_m \cdot \mathbf{u}_R) dS.$$

In the TM family, the expansion is

$$\begin{aligned} \mathbf{e}(\mathbf{r}, t) &= \sum_{m,n} v_{mn}(R, t) \text{grad}_s Y_{mn} \\ &\quad + \sum_{m,n} w_{mn}(R, t) \frac{Y_{mn}}{R} \mathbf{u}_R + w_o(R, t) \frac{1}{R\sqrt{4\pi}} \mathbf{u}_R \\ \mathbf{h}(\mathbf{r}, t) &= \sum_{m,n} i_{mn}(R, t) \mathbf{u}_R \times \text{grad}_s Y_{mn}. \end{aligned} \quad (34)$$

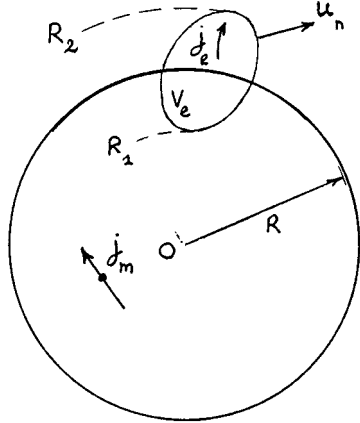


Fig. 4. Sources in free space.

Insertion in Maxwell's equations now yields (25)–(27), but without a source term in $\mathbf{u}_n \times \mathbf{e}$, and with $n(n+1)$ instead of k_m^2 . The only difference with (25)–(27) lies in the inclusion of a w_o coefficient, which represents the average radial component of \mathbf{e} over a spherical surface. The differential equation for w_o is

$$\varepsilon_o \frac{\partial w_o}{\partial t} = -\frac{1}{R\sqrt{4\pi}} \int_s (\mathbf{j}_e \cdot \mathbf{u}_R) dS. \quad (35)$$

The second member is different from zero between R_1 and R_2 only (Fig. 4). It is necessary to include the “ ψ_o ” term in (34) in order to expand in a *complete* set. In terms of fluxes, (23) still holds for the magnetic flux. Thus,

$$-\frac{\partial \phi_m(R, t)}{\partial t} = -\frac{\partial}{\partial t} \int_s (\mathbf{b} \cdot \mathbf{u}_R) dS = \int_s (\mathbf{j}_m \cdot \mathbf{u}_R) dS \quad (36)$$

but there is now an equivalent relationship for the electric flux, viz

$$-\frac{\partial \phi_e(R, t)}{\partial t} = -\frac{\partial}{\partial t} \int_s (\mathbf{d} \cdot \mathbf{u}_R) dS = \int_s \mathbf{j}_e \cdot \mathbf{u}_R dS = -\frac{\partial q_e}{\partial t} \quad (37)$$

where q_e is the electric charge contained in the sphere bounded by S . Note that (37) could have been obtained directly from the equation of conservation of charge by integrating

$$\operatorname{div} \left(\mathbf{j}_e + \frac{\partial \mathbf{d}}{\partial t} \right) = \operatorname{div} \mathbf{j}_e + \frac{\partial \rho}{\partial t} = 0 \quad (38)$$

over the sphere bounded by S . In Fig. 4, ϕ_e is zero up to $R = R_1$, after which its variation is governed by (37).

The following additional remarks are appropriate.

- 1) The term in ψ_o would be needed for the expansion of \mathbf{e} in a conical waveguide if the walls were *magnetic* instead of *electric*. In this dual situation, the roles of \mathbf{e} and \mathbf{h} are exchanged.
- 2) The electric currents \mathbf{j}_e may sometimes be advantageously replaced by equivalent magnetic currents \mathbf{j}_m (or conversely). The connection is through the relationship

$$\frac{\partial \mathbf{j}_m}{\partial t} = -\frac{1}{\varepsilon_o} \operatorname{curl} \mathbf{j}_e. \quad (39)$$

The value of $\mathbf{j}_m(\mathbf{r}, t)$ follows from a time integration of the second member, and consideration of the initial conditions on \mathbf{j}_e . Starting from $t = 0$, this operation is often written as

$$\mathbf{j}_m(\mathbf{r}, t) = -\frac{1}{\varepsilon_o} \int_o^t \operatorname{curl} \mathbf{j}_e(\mathbf{r}, \tau) d\tau = -\frac{1}{\varepsilon_o} \partial_t^{-1} \operatorname{curl} \mathbf{j}_e(\mathbf{r}, t). \quad (40)$$

Such a substitution is appropriate, for example, in replacing a frill of electric current (a small loop) by an equivalent magnetic dipole. The equivalence of the sources holds only for points outside the source volume V_e , and the curl should be understood in the sense of distributions. Thus (Fig. 4), for a piecewise continuous \mathbf{j}_e [4]

$$\operatorname{curl} \mathbf{j}_e = \{\operatorname{curl} \mathbf{j}_e\} + \mathbf{j}_e \times \mathbf{u}_n \delta_s \quad (41)$$

where the curly brackets indicate the (usual) curl at an interior point.

- 3) The ψ_o contribution obviously does not radiate. It represents reactive energy and is, therefore, important for the evaluation of the near field and Q of the sources. Radiation, therefore, finds its origin in the remaining terms of the expansion. The radiation problem boils down to the solution of a set of differential equations of the type

$$\frac{\partial^2 v}{\partial R^2} - \frac{1}{c_o^2} \frac{\partial^2 v}{\partial t^2} - \frac{n(n+1)}{R^2} v = f(R, t). \quad (42)$$

Such a detailed solution normally represents a major effort. Under time-harmonic conditions, spherical Bessel and Hankel functions are involved. The solution obtained with these functions can serve as a basis for solving (42) via an inverse Fourier transformation, which generates time-dependent multipoles [6]. The moments of the latter can also be evaluated directly by suitable integrations in the time domain. An example of such a nontrivial evaluation can be found in [1] and [2], where the source is a surface current

$$\mathbf{j}_s = \mathbf{j}_s(t) \mathbf{u}_x$$

flowing on a circular disk of radius a . The x -axis is a diameter of the disk. The pulse in that application is chosen as a twice-differentiated Gaussian

$$\mathbf{j}_s(t) = C e^{-(t/\gamma)^2} H_2 \left(\frac{t}{\gamma} \right)$$

with $\gamma = (12/7)^{1/2} T$, $H_2(x) = 4x^2 - 2$ and the pulselength

$$T = \frac{\int_{-\infty}^{\infty} j_s^2 t^2 dt}{\int_{-\infty}^{\infty} j_s^2 dt}.$$

The reader is referred to [1] and [2] for details. The dimensionless parameter $(a/c_o T)$ plays an important role in the analysis in that its value separates the “small” disks ($a \ll c_o T$) from the “large” ones ($a \gg c_o T$). A careful study of the convergence of the expansion shows that the number of modes needed is essentially three ($a/c_o T$).

APPENDIX

We expand $\operatorname{curl} \mathbf{e}$ in terms of the eigenfunctions and eigenvectors used for \mathbf{h} and j_m . Thus,

$$\begin{aligned} \operatorname{curl} \mathbf{e}(\mathbf{r}, t) &= \sum_m \alpha_m(R, t) \mathbf{u}_R \times \operatorname{grad}_s \phi_m + \sum_p \beta_p(R, t) \operatorname{grad}_s \psi_p \\ &= \sum_{p+o} \gamma_p(R, t) \frac{1}{R} \psi_p \mathbf{u}_R + \gamma_o(R, t) \frac{1}{R \sqrt{\Omega}} \mathbf{u}_R \end{aligned} \quad (43)$$

We shall evaluate, as an example, the β_p , γ_p , and γ_o coefficients (associated with the TE mode). Dot multiplying (43) with $\text{grad}_s \psi_p$ and integrating over S gives

$$k_p^2 \beta_p = \int_s \text{curl } \mathbf{e} \cdot \text{grad}_s \psi_p dS = \int_s \text{div}(\mathbf{e} \times \text{grad}_s \psi_p) dS - \int_s \mathbf{e} \cdot \text{curl} \text{grad}_s \psi_p dS$$

but $\text{curl} \text{grad}_s \psi_p = 0$ and

$$\text{div}(\mathbf{e} \times \text{grad}_s \psi_p) = \text{div}_s(\mathbf{e} \times \text{grad}_s \psi_p) + \frac{\partial}{\partial R} \mathbf{u}_R \cdot (\mathbf{e} \times \text{grad}_s \psi_p).$$

Since

$$\int_s \text{div}_s dS = \int_c (\mathbf{u}_n \cdot \mathbf{a}) dc$$

holds for a tangential vector function $\mathbf{a}(\theta, \varphi)$, we find

$$\beta_p = \frac{\partial v_p}{\partial R} + \frac{1}{k_p^2} \int_c (\mathbf{u}_n \times \mathbf{e}) \cdot \text{grad}_s \psi_p dc.$$

In the next step, we dot multiply (43) with $(1/R)\psi_p$ and $1/R\sqrt{\Omega}$ to obtain after integration

$$\begin{aligned} R\gamma_p &= \int_s (\mathbf{u}_R \cdot \text{curl } \mathbf{e}) \psi_p dS \\ &= \int_s \psi_p \text{div}(\mathbf{e} \times \mathbf{u}_R) dS \\ &= \int_s \psi_p \text{div}_s(\mathbf{e} \times \mathbf{u}_R) dS \\ &= \int_s \text{div}_s(\psi_p \mathbf{e} \times \mathbf{u}_R) dS - \int_s \text{grad}_s \psi_p \cdot (\mathbf{e} \times \mathbf{u}_R) dS. \end{aligned}$$

Hence,

$$\gamma_p = \frac{1}{R} \int_c (\mathbf{u}_n \times \mathbf{e}) \cdot \psi_p \mathbf{u}_R dc + k_p^2 v_p.$$

Similarly,

$$\gamma_o = \frac{1}{R\sqrt{\Omega}} \int_c (\mathbf{u}_n \times \mathbf{e}) \cdot \psi_o \mathbf{u}_R dc.$$

Insertion of (43) into Maxwell's equation in curle leads immediately to (18), (20), and (21).

REFERENCES

- [1] A. Shlivinski and E. Heyman, "Time-domain near-field analysis of short-pulse antennas—Part I: Spherical wave (multipole) expansion," *IEEE Trans. Antennas Propagat.*, pt. , vol. 47, pp. 271–279, Feb. 1999.
- [2] ———, "Time-domain near-field analysis of short-pulse antennas—Part II: Reactive energy and the antenna Q ," *IEEE Trans. Antennas Propagat.*, vol. 47, pp. 280–286, Feb. 1999.
- [3] J. Van Bladel, "Contribution of the ψ -constant mode to the modal expansion in a waveguide," *Proc. Inst. Elect. Eng.*, pt. H, vol. 128, pp. 247–251, 1981.
- [4] ———, *Singular Electromagnetic Fields and Sources*. Oxford, U.K.: Clarendon, 1991, p. 25, 48, 109, 175.
- [5] ———, *Electromagnetic Fields*. New York: McGraw-Hill, 1964, p. 26, 241, 502, 504.
- [6] E. Heyman and A. J. Devaney, "Time-dependent multipoles and their application for radiation from volume source distributions," *J. Math. Phys.*, vol. 37, pp. 682–692, 1996.

Six-Port Self-Calibration Based on Active Loads Synthesis

Toshiyuki Yakabe, Fadel M. Ghannouchi, Eid E. Eid, Kohei Fujii, and Hatsuo Yabe

Abstract—An automatic method for self-calibrating six-port reflectometers is reported in this paper. It is based on the use of an active impedance synthesis system. This self-calibration method allows a completely autonomous operation, reduces measurement errors caused by the frequent connecting and disconnecting of calibration standards, and is suitable for low and high frequencies, where sliding shorts are difficult to manufacture. In addition, it simplifies operation of six-port reflectometers to nonspecialized users. The experimented impedance synthesis presented relies on an in-phase and quadrature vector modulator, and the entire system is computer controlled.

Index Terms—Microwave measurement, self-calibration, six-port.

I. INTRODUCTION

In order to calibrate a six-port reflectometer at a given frequency, many different loads, such as short circuit, matched load, and set of delay lines, have to be connected successively to the measuring port [1]. In theory, 5-1/2 loads are needed to find the junction parameters, but for experimental considerations, the 13 standards method [1] is usually adopted, where 13 unknown different loads have to be connected to the measuring port of the six-port junction.

Thus, automating these procedures requires being able to synthesize many different loads at the measuring port of the six-port junction. Such synthesis can be accomplished using an automated passive impedance tuner systems such as those described in [2] and [3]. However, due to the finite insertion losses, a perfect open or short circuits cannot be obtained, especially at high frequencies. In this paper, we propose a method to avoid such difficulty by using an active loads approach [4], [5]. This method allows synthesis of any load (even outside the unit circle) over the Smith chart for calibration purposes. With this method, all operations that are inherent to the reflectometer such as junction calibration, become invisible to the user, leaving only a simple experimental procedure for error-box measurements [1] to be done, as in standard network analyzers.

II. SYSTEM DESCRIPTION

Six-port reflectometers are usually used for finding the reflection coefficient of a load placed at the measuring port of the six-port junction. Six-port theory [1] shows that this complex coefficient is directly related to the microwave power at each of the four auxiliary ports. By normalizing these quantities with respect to the reference port, we end up with three power ratios that can be used to compute the unknown reflection coefficient.

The block diagram of the system used is shown in Fig. 1. It consists of the six-port reflectometry system (six-port junction, Schottky diode detectors, and CPU) and the controllable vector modulator (or a phase shifter and an attenuator). The incoming signal from the source is split in two parts using a two-way power divider. One of them feeds port 1

Manuscript received October 4, 1999; revised December 24, 2000.

T. Yakabe and H. Yabe are with the Department of Information and Communication Engineering, University of Electro-Communications, Tokyo 182-8585, Japan (e-mail: yakabe@ice.uec.ac.jp).

F. M. Ghannouchi and E. E. Eid are with the Electrical and Computer Engineering Department, Ecole Polytechnique, Montreal, QC, Canada H3C 3A7.

K. Fujii is with the Japan Radio Company Ltd., Tokyo 181-8510, Japan.

Publisher Item Identifier S 0018-9480(02)03028-4.